©2016 Published in 4th International Symposium on Innovative Technologies in Engineering and Science 3-5 November 2016 (ISITES2016 Alanya/Antalya - Turkey)

AN ACCURATE LINE DETECTION BY A NOVEL LINE FOLLOWER SENSOR OUTPUT PROCESSING METHOD

[*1]Gökhan Dındış and [2]Abdurahman Karamancıoğlu
[*1,2]Eskişehir Osmangazi University, Engineering-Architecture Faculty,
Department of Electrical-Electronics Engineering, 26040 Eskişehir, Turkey

Abstract :

Line sensors are widely used in line following robots. Their performances are at a premium in the line following task of Automated Guided Vehicles (AGV) at hobby or industrial scale. In this manuscript a a line following sensor (LFS) array output processing method that significantly enhancing the performance of the LFS array is presented. This processing method makes use of cubic Bezier curves and extracts in a highly accurate position information from the LFS outputs. A line sensor array configuration under consideration consists of M sets of infrared (IR) emitting LED and IR sensitive photodetector, called an L-Pd set. The sets are equispaced and collinearly positioned. In the mode of operation light from the IR emitting LEDs is reflected back onto the photosensitive detectors. Depending on the intensity of the light received, each photodetector outputs an analog voltage between Vmin to Vmax volts. Because the L-Pd set components are possibly not identical, each one's voltage response to all-black, respectively all-white, targets are not equal. Normalization of the L-Pd sets is achieved by the aid of linear parametrizing. Having the normalized L-Pd sets the remaining problem can be stated as detecting the center of a black line strip placed on a white background by analyzing the voltage outputs of the L-Pd sets in the line sensor array. At this stage of the problem the voltage outputs of the L-Pd sets versus the sensor locations is formed, and transformed into a sequence cubic Bezier curves. An efficient algorithm presented in this manuscript yields the center of the black strip. An experimental set–up presented in this manuscript shows validity and accuracy of the approach outlined above.

Key words: Line follower sensor, reflective sensor, Bezier Curves, AGV control

1. Introduction

Line sensor array is an essential component of line tracking robots. Mainly it is designed to detect a line drawn on a floor. Besides the line tracking, the line sensor array may also be used in motion detection and proximity sensing problems. Improvements in the line sensor processing therefore have a wide impact in the aforementioned fields. In this manuscript the line sensor data is calibrated and processed by a novel algorithm which uses cubic Bezier curves as its main tool. Experimental verifications presented in the sequel show that the proposed approach is computationally efficient and yield fairly precise results.

A line sensor array configuration under consideration consists of *M* sensors in which each sensor has an infrared (IR) emitting LED and IR sensitive photodetector. Operation principle of a sensor is as follows: Current through the LED, within specified values, causes light emitting which reflects back upon hitting a surface. The photodetector (generally a phototransistor) detects intensity of the reflected light and a current flow is generated based on its intensity. A voltage

*Corresponding author: Address: Faculty of Eng., Dept. of Electrical & Electronics Eng., Osmangazi University, 26480, Meselik, Eskisehir TURKEY. E-mail address: gdindis@ogu.edu.tr, Phone: +90.222.239.3750/3283

caused by this current in a circuit is measured electronically and used for any required purpose. Figures 1a and 1b shows the operation of a reflective sensor device and its basic circuitry respectively.

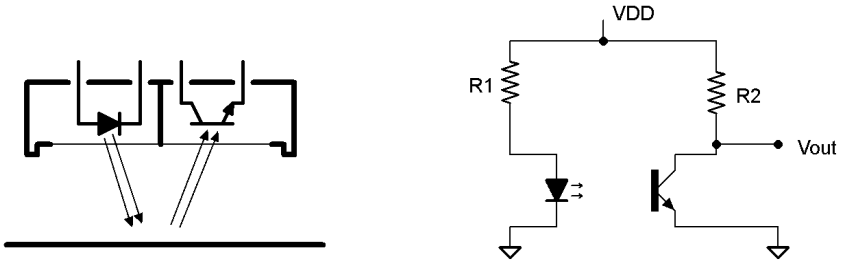

(a) (b)

Figure 1 Operation diagram and a basic circuitry for a reflective sensor

We in the sequel employ the notation L-Pd for an IR LED and photodetector pair. These sensors are positioned collinearly with spacing between each one is *d* units (See Figure 2). During the mode of operation each IR LED emits signal and measures its reflection.

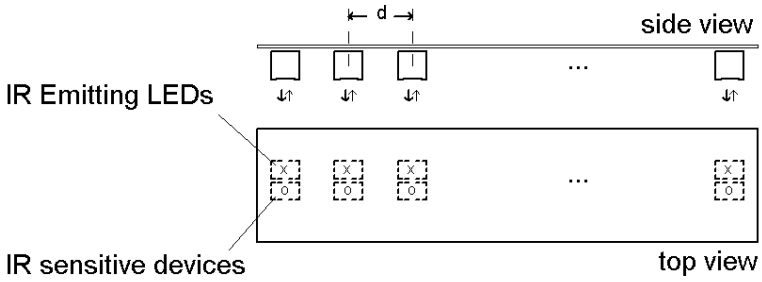

Figure 2 A representative diagram of a line sensor array

To gain an insight in working principles of a sensor array we may consider the configuration in Figure 3-a in which a detector moves on a straight strip having white background and a crossing black strip on it. Figure 3-b shows that voltage output of the detector gets lower as reflection comes from a brighter surface.

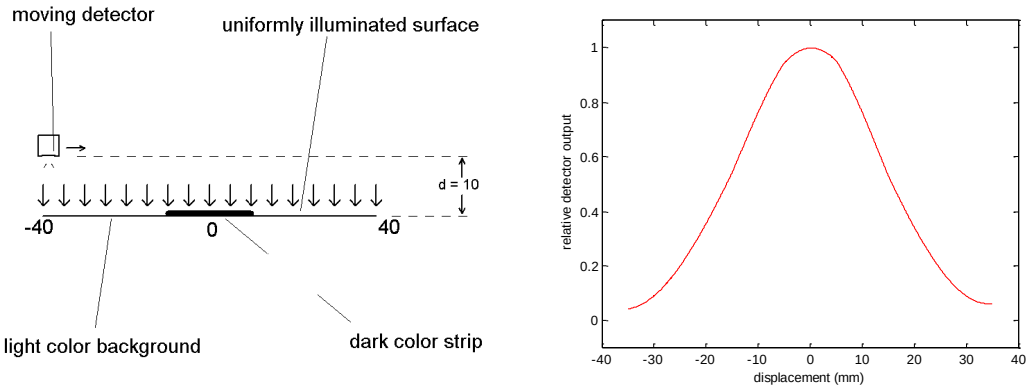

(a) (b)

Figure 3 Uniformly illuminated surface and its normalized outputs

Since a moving detector requires additional hardware, it is costly and not practical; a similar functioning is obtained with a sliding black strip below a fixed line sensor array (See Figure 4-a). Figure 4-b shows that the discrete data corresponding to the sensors are used in a fitting curve to obtain a similar graphics. This graphics is the basis for generating the line position. The proposed approach of this manuscript detects center of the line by evaluating its graphics.

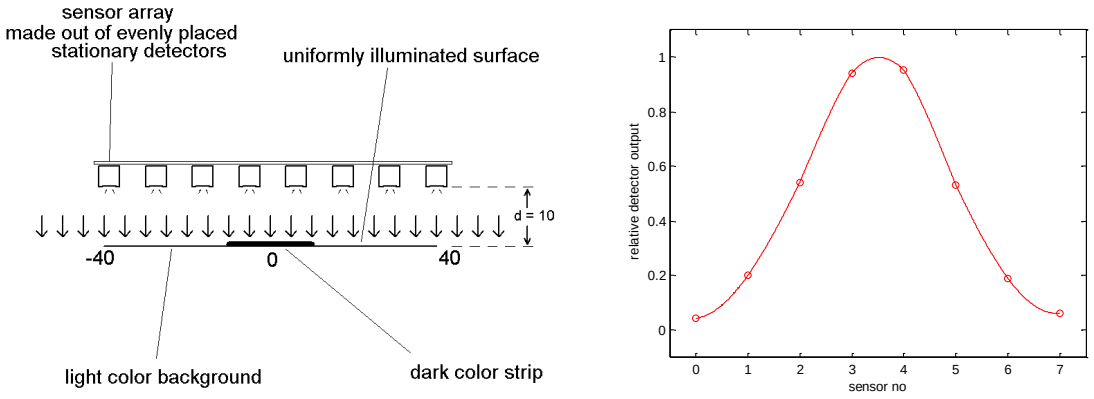

(a) (b)

Figure 4 A reflective sensor array and its discrete outputs

One of the major problems encountered in line sensor operations is its non-identical L-Pd components. The non-identical IR LEDs lead to a unevenly illuminated field which gives local variations in the reflection pattern. Such local variations cause wrong position predictions. It can be experimentally verified that photodetectors suffer the same problem; they are, in general, non-identical. A properly designed circuit shown in Figure 5 handle both issues, by adjusting each LED's current transfer ratio to emit the same candle output as the other ones and by tuning up each detector with the potentiometers to get same voltages for the same amount of light inputs. However, this circuitry has more manufacturing costs and needs more labor before operations, consequently, it is not practical. Using the commercially existing sensor array configurations with a software to be introduced in this manuscript is practical, and eliminates the problems arising from non-identicality. It will be shown that a proper software eliminates deteriorating effects of the external disturbances which have not mentioned above. For instance, environmental fluctuations always should be under consideration in most applications. As sun is the major external IR source around, sunny or cloudy days, shaded or unshaded work areas make significant differences on readings. Besides, nonlinearity per current transfer ratios for each component may differ from each other in some level, and all parameters change with temperature at some extent too [1,2]. Another justification of the software based calibration is that the time degrading of the optic components most likely shift the calibration values if they were calibrated by hardware. In Section 4 we introduce a soft calibration technique that eliminates the aforementioned deficiencies of the commercially existing line sensor arrays.

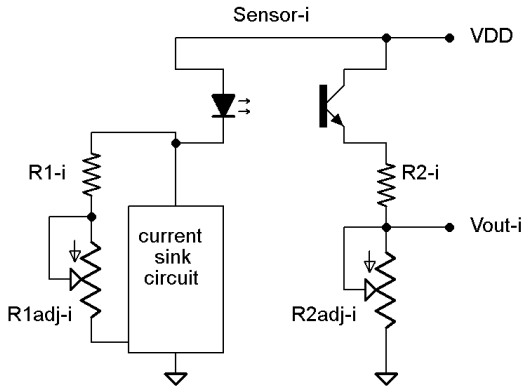

Figure 5 A proper circuit for a single cell of the reflective line sensor array

Popularity of line tracking robots, due to their usages in manufacturing plants and in competitions, motivates researchers to improve its performance. In this regard, its essential component, line sensors array, attracts the main attention. In [3,4], a teaching platform for mobile robots is built. Line sensors taking place in the mobile robots' hardware is calibrated using a linear approximation. Following this, among the 8 sensors forming the line sensor array three of them with the highest output are used in a quadratic polynomial fitting. The point where this quadratic polynomial attains the maximum is output as the line position. In the present manuscript all available data are used for graphing the light detected. However, in detecting the line position, the present manuscript uses outputs of four sequential sensors with highest output values. In [5], defining error as deviation from the center of the line, it is calculated by dividing the weighted average of the sensor readings by the average value and normalizing the value. In [6] a line tracking robot is designed where its sensors are placed in a way to detect the junctions besides the line itself.

In the next section, a brief review of the main tool, cubic Bezier curves, is given. In the 3rd section the line sensor configuration under consideration is described. In the 4th section, the proposed sensor calibrations and line detecting procedure is presented. The 5th section is devoted to the experimental results and their interpretations. The last section has the concluding remarks.

2. A Brief Review of Cubic Bezier Curves

A planar cubic Bezier function $P(u) := \big(x(u), y(u)\big),\ 0 \le u \le 1$, is completely specified with four control points (C_0, C_1, C_2, C_3) corresponding to the parameter values $(0, u_1, u_2, 1)$. The P values corresponding to these u parameters are denoted by (P_0, P_1, P_2, P_3). The control points C_0 and C_3 equal P_0 and P_3 respectively. However, the control points C_1 and C_2 are not necessarily equal to P_1 and P_2; C_1 and C_2 are on the tangent lines passing through P_0 and P_3 respectively, that is, $C_1$is the direction of the curve at P_0, and C_2 is the opposite of curve's direction at P_3. The cubic Bezier curve in terms of the control points is written as [7,8]

$$P(u) = (1-u)^3 C_0 + 3(1-u)^2 u C_1 + 3(1-u)u^2 C_2 + u^3 C_3, \;\; u \in [0,1] \quad (1)$$

where $(1-u)^n u^{3-n}, \; n = 0,1,2,3$, are called Bernstein basis polynomials for a cubic Bezier function.

3. The Line Sensor Configuration

In practice a line sensor array is mounted below a vehicle and as vehicle moves the sensor array swipes the surface having the black strip (Figure 6-a). For convenience, an identification number is assigned to each sensor. The id numbers 0 to M-1 is assigned to the sensors from left to right, and sensor reading corresponding to the k-th sensor is denoted by s_k. As any sensor gets closer to the black line on a white background, its reading tends to its highest value. The line sensor array is fixed below a line tracking vehicle, and black line on a white background is implemented on a table (Figure 6-b).

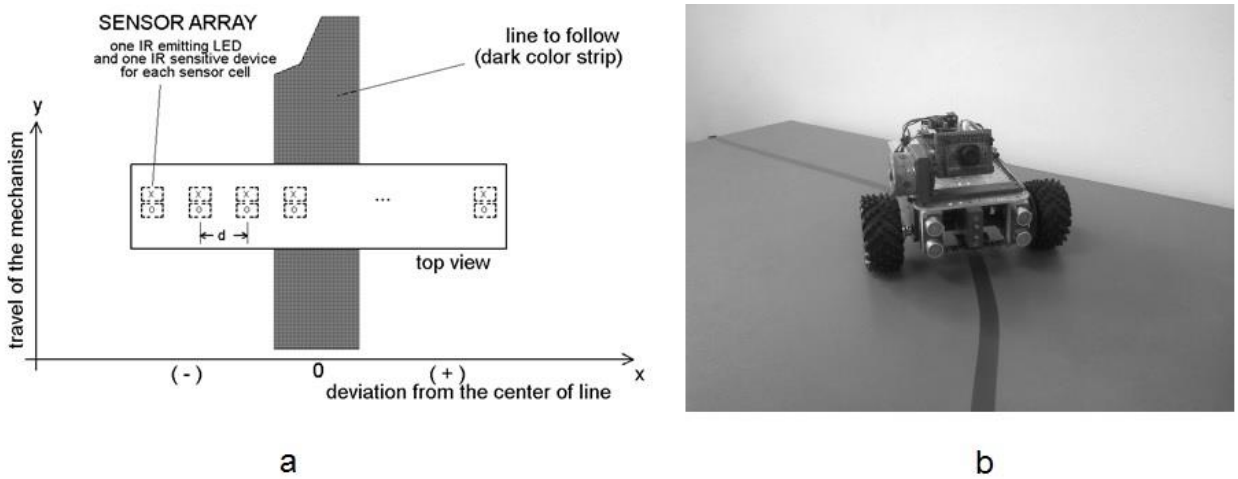

Figure 6. A line detection configuration and its a photo after mounting on the experimental vehicle

4. Sensor Calibration and Line Detection Method

As mentioned in previously, the sensors in the line sensor array are not identical in practice. Each one may have a different minimum and maximum output values. Most approaches, as the one in our method, require normalization of sensor readings. We linearly parametrize each sensor output where each one's lowest and highest output values correspond 0 and 1 respectively. Specifically, lowest and highest readings s_{k_min} and s_{k_max} yield the parametrized output

$$s_k(p) = (1-p)s_{k\_min} + p\, s_{k\_max}, \;\; 0 \le p \le 1 \quad (2)$$

Noting that sensors are non-identical and sensitive to environmental conditions we design an on-site calibration process which involves sliding a black strip forward once below the sensors. Its principal diagram is shown below in Figure 7.

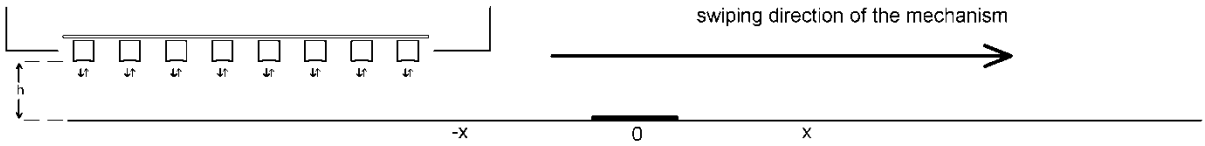

Figure 7 A novel on-site calibration technique

For the on-site calibration, assuming that the line sensor array is positioned above a white background, sliding a black strip below the array makes every sensor output achieve its all possible values including the minimum and maximum. This process takes environmental light and temperature into account, and results a higher signal to noise ratio (SNR) in the calibration.

We further improve the SNR by applying more intense IR LED to the platform so that in the reflected light detected by photodetectors the effects of the environmental light is reduced. Each IR LED in the sensor array is allowed to be driven by maximum 25 mA for a continuous operation. In our process we drive each IR LED by 100 mA with 25 % duty cycles, which increases the light intensity level significantly and does not harm the LEDs. Sensors' minimum and maximum values so obtained, namely, s_{k_min} and s_{k_max} $k = 0, \ldots, M-1$, are used in Expression (2) for the normalization. Thus, using (2), any actual measurement corresponds a parameter value between 0 and 1. At this point we may explain the reasoning for not choosing a duty cycle less than 25 % for the sake of a larger LED current. It may be speculated that using a larger LED current would increase the SNR further. It may sound good but sensor's component characteristics shown below in Figure 8 indicates that the LED's light emitting settles almost in 15 milliseconds. If a LED current pulse is shorter than this time period the LED light would not reach its steady state value, and its reflections do not serve the purpose.

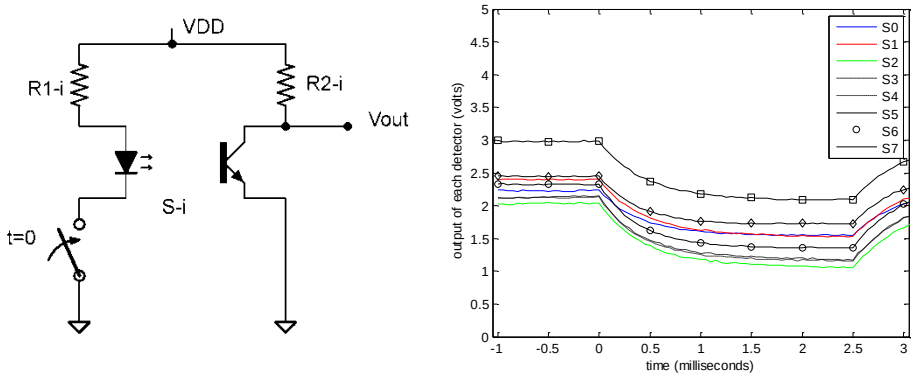

Figure 8. A simple pulsed current circuit and output responses of the detectors

The line detection algorithm to be presented below is based on calibrated sensor representations. Let the M sensor readings be $s_0, s_1, \dots, s_{M-1}$. In the CBC domain it may be represented by M-3 overlapping cubic Bezier curves. For this representation the readings are grouped as

$$(s_0, s_1, s_2, s_3), (s_1, s_2, s_3, s_4), (s_2, s_3, s_4, s_5), \dots, (s_{M-4}, s_{M-3}, s_{M-2}, s_{M-1}). \quad (2)$$

Each group contains 4 consecutive elements corresponding to 4 neighboring sensor readings. We represent each group by a cubic Bezier curve. By this, except the leftmost and rightmost intervals, every spatial interval between every two consecutive sensors is CBC represented by the readings coming from the two sensors on its left and the two sensors on its right. The leftmost and the rightmost intervals are respectively represented by the first and last groups in (2). Using the relevant CBC data for every interval, sensor readings data versus sensor positions form a continuous graphics. This manuscript, besides forming this graphics by using CBC formulation, provides an algorithmic interpretation for detection of the center of the line.

5. Experimental Results

The line sensor card used in the experiments is a commercially available card named Pololu qtr8a. It has 8 sensors on it, and the distance between the sensors is *0.4* inch. Even though *M=8* and *d=0.4* inch is used in the experiments, the proposed approach of this manuscript is valid for any $M \geq 3$ and for any physically meaningful *d*. We let d be normalized and unit-free for the sake of simplicity in the presentation.

Our In the sensor calibration phase, we did one swipe as in the configuration shown in Figure 7. One swipe takes 5 seconds and making 100 readings per second results in 500 readings in one swipe. Figures 9-a and 9-b show the first reading and the first 500 readings respectively. For the sake simplicity in perception the data read are connected by linear line segments. Inspecting Figure 9-b, one can visually see the minimum and maximum voltage values returned by the sensors before the calibration.

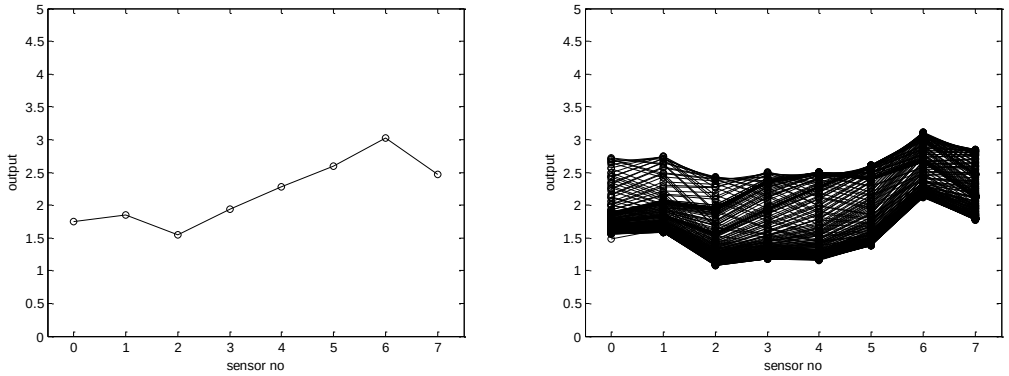

(a) (b)

Figure 9 Swiped readings at the beginning and during 500 readings (100 readings/second)

To present the benefits of using cubic Bezier curve connection of the data points, we do an experiment that results one reading of each sensor corresponding to some position of black strip below the sensor array. These data points are connected by linear line segments and superimposed on the graphics of reading boundaries obtained from Figure 9-b. The resulting graphics is shown in Figure 10.

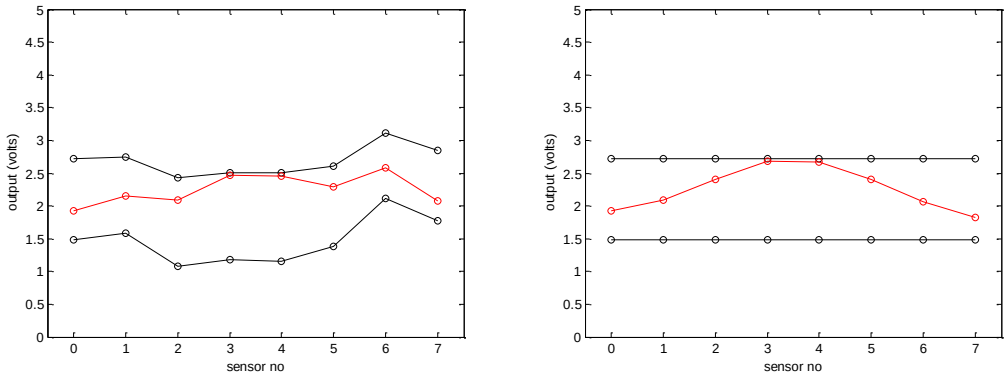

Figure 10 Before and after the calibration process: top and bottom shows maximum and minimum values respectively, after 500 readings of swiping; another value set just taken after this shown superimposed when the sensor is almost at the center

The calibrated version of the boundaries together with a reading connected by cubic Bezier curves are shown in Figure 11. This CBC connected data corresponding to one reading is now ready for an accurate detection of the black line strip.

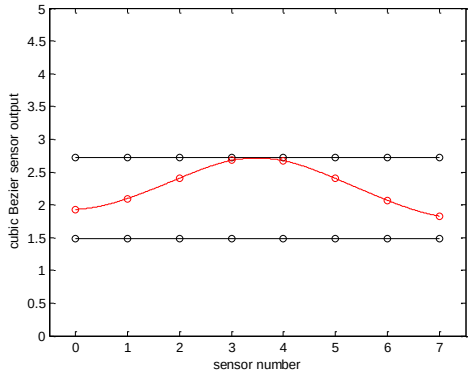

Figure 11 CBC connected data corresponding to one calibrated reading.

In forming the graphics, as mentioned in the previous section, we fit cubic Bezier curves to the data grouped in successive four sensors. Figure 12 shows first, second, third, and last groups and their validity on the curve in bold line for an illustration.

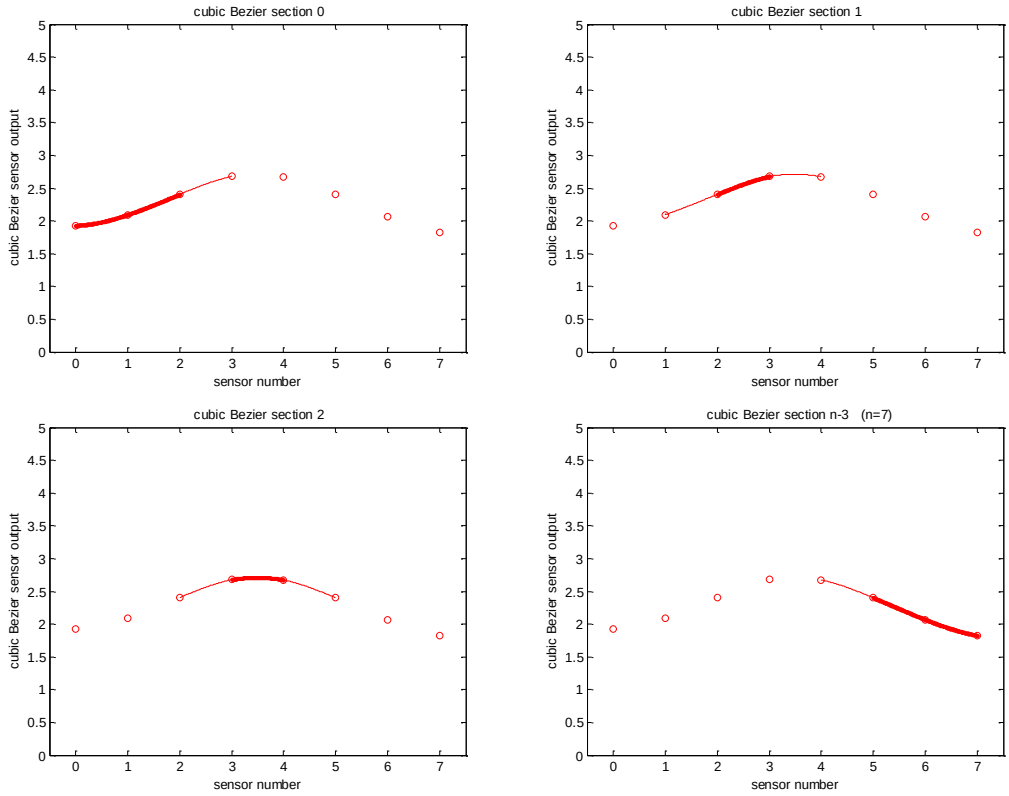

Figure 12. Sensor groupings and their validity segments

In detecting the black line center we use the readings of four sensors with highest readings as shown in Figure 13. In the experiments denoting the readings a sequential four sensors by $s_i = b_0, s_{i+1} = b_1$, $s_{i+2} = b_2$, and $s_{i+3} = b_3$ corresponding cubic Bezier curve parametrization is obtained as

$$S(u) = (-4.5b_0+13.5b_1-13.5b_2+4.5b_3)u^3 + (9b_0-22.5b_1+18b_2-4.5b_3)u^2 + (-5.5b_0+9b_1-4.5b_2+b_3)u + b_0$$

Its derivative

$$\dot{S}(u) = (-13.5b_0+40.5b_1-40.5b_2+13.5b_3)u^2 + (18b_0-45b_1+36b_2-9b_3)u + (-5.5b_0+9b_1-4.5b_2+b_3) = 0$$

has a root in the interval [0,1], calculated by the quadratic root finding formula, yields the position of the black line strip. Since, in our framework, four neighboring sensors, say i-th through $i + 3^{rd}$, are used to create a Bezier curve, $u = 0$ and $u = 1$ coincide with the positions of i-th and $i + 3^{rd}$ sensors; and intermediate values of the u parameters correspond positions between them.

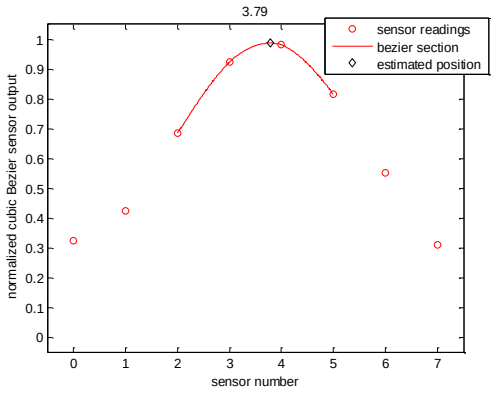

Figure 13. Cubic Bezier curve corresponding to the highest four readings

Conclusions

A novel line sensor array output processing method that enhances its line detection accuracy is presented. The method soft-calibrates the possibly non-identical sensor characteristics, and uses cubic Bezier curves as its major tool in graphing the spatially varying values of the sensor readings. Experimental results are included to illustrate validity of the proposed approach.

References

[1] CNY70 – Reflective Optical Sensor with Transistor output. Vishay Electronic GmbH, Rev. 1.8, 30-Jul-12 [online]. Available: http://www.vishay.com/docs/83751/cny70.pdf

[2] QRE1113, QRE1113GR Miniature reflective object sensor. Fairchild Semiconductor Corp., Rev.2.7, Apr.2016 [online]. Available: https://www.fairchildsemi.com/datasheets/qr/qre1113.pdf

[3] Lee C-S, Su J-H, Lin K-E, Chang J-H, Chiu M-H, Lin G-H. A Hands-on laboratory for autonomous mobile robot design courses. Proc 17th Inter Federation of Automatic Control World Congress, Korea, 2008; p. 9743-9748.

[4] Su J-H, Lee C-S, Huang H-H, Chuang S-H, Lin C-Y. An intelligent line-following robot project for introductory robot courses. World Transactions on Engineering and Technology Educ., Wiete 2010; 8, 4: p. 455-461.

[5] Balaji V, Balaji M, Chandasekaran M, Ahamed Khan MKA, Elemvazuthi I. Optimization of PID control for high speed line tracking robots. Procedia, 2015; 76, p. 147-154.

[6] Poyen F, Guin S, Deep M. Secured robotic line follower vehicle. Proceedings of the Intl. Conf. on Innovative Trends in Electronics Communication and Applications (ICIECA2013); pp.9-16.

[7] Farouki RT. The Bernstein polynomial basis: A centennial retrospective. Comput Aided Geom D. 2012; 29: p. 379-419.

[8] Yamaguchi F. Curves and Surfaces in Computer Aided Geometric Design. Springer Verlag; 1988.